1521-0103/381/3/247–256$35.00
THE JOURNAL OF PHARMACOLOGY AND EXPERIMENTAL THERAPEUTICS

dx.doi.org/10.1124/jpet.121.001019
J Pharmacol Exp Ther 381:247–256, June 2022

The Journal of PHARMACOLOGY And Experimental Therapeutics

Anisodamine Enhances Macrophage M2 Polarization through Suppressing G9a-Mediated Interferon Regulatory Factor 4 Silencing to Alleviate Lipopolysaccharide-Induced Acute Lung Injury[S]

Yunfeng Zhang, Dingli Song, Ziyang Peng, Rui Wang, Kai Li, Hong Ren, Xin Sun, Ning Du, and Shou-Ching Tang

Department of Thoracic Surgery, The First Affiliated Hospital of Xi'an Jiaotong University, Xi'an, China (Y.Z., D.S., Z.P., R.W., K.L., H.R., X.S., N.D.) and Cancer Center and Research Institute, University of Mississippi Medical Center, Jackson, Mississippi (S.-C.T.)

Received November 15, 2021; accepted March 31, 2022

ABSTRACT

Acute lung injury (ALI) is a serious inflammatory lung disease. Imbalances in the polarization of classically activated (M1) and alternatively activated (M2) macrophages are closely related to ALI. Anisodamine has a promising therapeutic effect for septic shock. Nevertheless, the role of anisodamine in progression of ALI remains to be investigated. Our results showed that anisodamine significantly reduced lung damage, myeloperoxidase (MPO) activity, lung wet/dry ratio, total cell number, and protein concentrations in bronchoalveolar lavage fluid and decreased interleukin (IL)-6 level and the levels of M1 phenotypic markers, whereas it increased IL-10 level and the levels of M2 phenotypic markers in mice with a nasal instillation of lipopolysaccharide (LPS). Bone marrow–derived macrophages (BMDMs) were stimulated or transfected with LPS plus anisodamine or LPS plus G9a short hairpin RNA. Anisodamine and downregulation of G9a both promoted BMDM M2 polarization caused by IL-4 treatment and inhibited M1 polarization resulting from LPS treatment. Chromatin immunoprecipitation assay revealed that anisodamine inhibited G9a-mediated methylation and expression suppression on interferon regulatory factory 4 (IRF4). Overexpression of G9a or silence of IRF4 reversed the improvement effect of anisodamine on lung tissue injury, evidenced by an increase of MPO activity and the restoration of LPS-induced alterations of M1 and M2 polarization. In conclusion, anisodamine protected against LPS-induced ALI, during which anisodamine suppressed the LPS-stimulated alterations of macrophage M1 and M2 polarization through inhibiting G9a-mediated methylation of IRF4, suggesting that anisodamine was a potential therapeutic drug to alleviate ALI.

SIGNIFICANCE STATEMENT

Anisodamine treatment was able to attenuate lung injury and pulmonary edema caused by lipopolysaccharide (LPS) stimulation, and the specific mechanism was that anisodamine reversed the LPS-induced alterations of M1 and M2 polarization by inhibiting G9a-mediated methylation and expression suppression of interferon regulatory factor 4, which suggests that anisodamine has the potential to alleviate acute lung injury.

Introduction

Acute lung injury (ALI) is a respiratory disease that was characterized by infiltration of inflammatory cells, overproduction of inflammatory mediators, rapid alveolar damage, and cytokine accumulation, leading to serious acute respiratory distress syndrome (ARDS) (Li et al., 2016; Nie et al., 2019). ARDS and ALI are respiratory diseases with high mortality rates, and despite significant advances in therapeutic strategies and understanding of the associated respiratory physiology, in critically ill patients, morbidity and mortality from ALI and ARDS remain high (Xie et al., 2018). However, due to the unsatisfactory efficacies of the currently therapeutic methods for ALI/ARDS, there is necessity to discover and develop effective therapeutic drugs.

Altered alveolar macrophage (AM) activation is considered a major contributor to the progression of uncontrolled acute lung inflammation in ALI/ARDS patients, and studies reported that macrophages exert exclusive functions in the procession of inflammation during ALI/ARDS (Huang et al., 2018; Li et al., 2018a). Alveolar macrophages are considered the main immune cells in the initiation and resolution phases of ALI/ARDS (Laskin et al., 2019). Macrophages, as a highly

No author has an actual or perceived conflict of interest with the contents of this article.
dx.doi.org/10.1124/jpet.121.001019.
[S] This article has supplemental material available at jpet.aspetjournals.org.

ABBREVIATIONS: ALI, acute lung injury; AM, alveolar macrophage; ARDS, acute respiratory distress syndrome; BALF, bronchoalveolar lavage fluid; BMDM, bone marrow–derived macrophage; H3K, histone-3-lysine; IL, interleukin; IRF4, interferon regulatory factor 4; KLF, Kruppel-like factor; LPS, lipopolysaccharide; M1, XXX; M2, XXX; MPO, myeloperoxidase; shRNA, short hairpin RNA; STAT, signal transducer and activator of transcription.

plastic and heterogeneous cell population, functional differences were distinctly exhibited under different microenvironments in vitro and in vivo and polarize into different phenotypes. Two phenotypes are observed when the macrophages are activated, including the classically activated (M1) phenotype and the alternatively activated (M2) phenotype (Qiu et al., 2021). After exposure to pathogens, resting macrophages (M0) mainly differentiate into proinflammatory phenotype (M1) and anti-inflammatory phenotype (M2), depending on the different microenvironment (Song et al., 2019). To respond to interferon-γ, lipopolysaccharide (LPS), or other cytokines, M1 macrophages secrete a large number of proinflammatory cytokines including tumor necrosis factor α, interleukin (IL)-6, and IL-1β to enhance the inflammation response and recruit neutrophils to the alveolar space (Rőszer, 2015), thus encouraging inflammation to mediate tissue damage, tissue regeneration, and wound healing. After being stimulated with several factors including IL-4, IL-10, and IL-13, M2 macrophages could be activated to inflammation resolution and tissue repair, compared with M1 (Wang et al., 2019). In ALI, the proportion of M1 macrophages, neutrophil recruitment, and secretion of numerous cytokines were increased at the acute inflammatory phase (Lin et al., 2020). The dynamic changes in the balance and function of M1/M2 macrophage subsets have a significant impact on inflammatory responses (Zhou et al., 2020). Increasing evidence has shown that the modulation of macrophage polarization could improve lung injury by changing the alterations of macrophage M1 and M2 phenotypes (Ren et al., 2021). Therefore, effectively controlling macrophage activation and differentiation will help regulate macrophage initiation and may be a potential approach to treat ALI/ARDS.

Anisodamine, an alkaloid obtained from *Anisodus sp.*, is commonly used for gastrointestinal spasms and organophosphate pesticide poisoning (Li et al., 2020a). Studies have reported that anisodamine has significant anti-inflammatory effects, inhibits oxidative stress and apoptosis of cardiomyocytes, and has cardioprotective effects against myocardial ischemia/reperfusion injury in rats (Yao et al., 2018). Anisodamine attenuates rhabdomyolysis resulting from acute kidney injury through suppressing endoplasmic reticulum stress–associated TXNIP/NLRP3 inflammasome (Yuan et al., 2017). Anisodamine exerted anti-inflammatory effects in animal models and even in patients with ALI (Guoshou et al., 2013; You et al., 2014; Zhao et al., 2021), but the potential regulatory mechanism of anisodamine on the alterations of macrophage polarization phenotypes in ALI remains unclear.

Although anisodamine and M2 macrophages are favorable for ALI treatment, the role of anisodamine in macrophage polarization is unclear, especially on M2. Thus, we investigated the therapeutic effects of anisodamine on ALI resulting from LPS and whether anisodamine regulates the differentiation of macrophages. Finally, we revealed a mechanism by which anisodamine reversed the alterations of macrophage M2 polarization induced by LPS in vitro.

Materials and Methods

Establishment of the ALI Animal Model. A total of 48 male C57BL/6 mice (aged 6–8 weeks, weighting 18–23 g) were obtained from the Medical Experimental Center of Xi'an Jiaotong University and maintained in a controlled environment with an air-conditioned atmosphere at 25°C and a 12-hour light/dark cycle. The animal experiments in this study were conducted in accordance with the National Institutes of Health Guide for the Care and Use of Laboratory Animals and were approved by the Ethics Committee of the First Affiliated Hospital of Xi'an Jiaotong University (XJTULAC-2019-173). All mice were randomly divided into six groups (n = 8 per group) as follows: control group, LPS group, LPS + anisodamine group, LPS + anisodamine + vector + short hairpin RNA (shRNA) group, LPS + anisodamine + G9a + shRNA group, and LPS + anisodamine + vector + interferon regulatory factor 4 (IRF4) shRNA. The model of ALI mice was

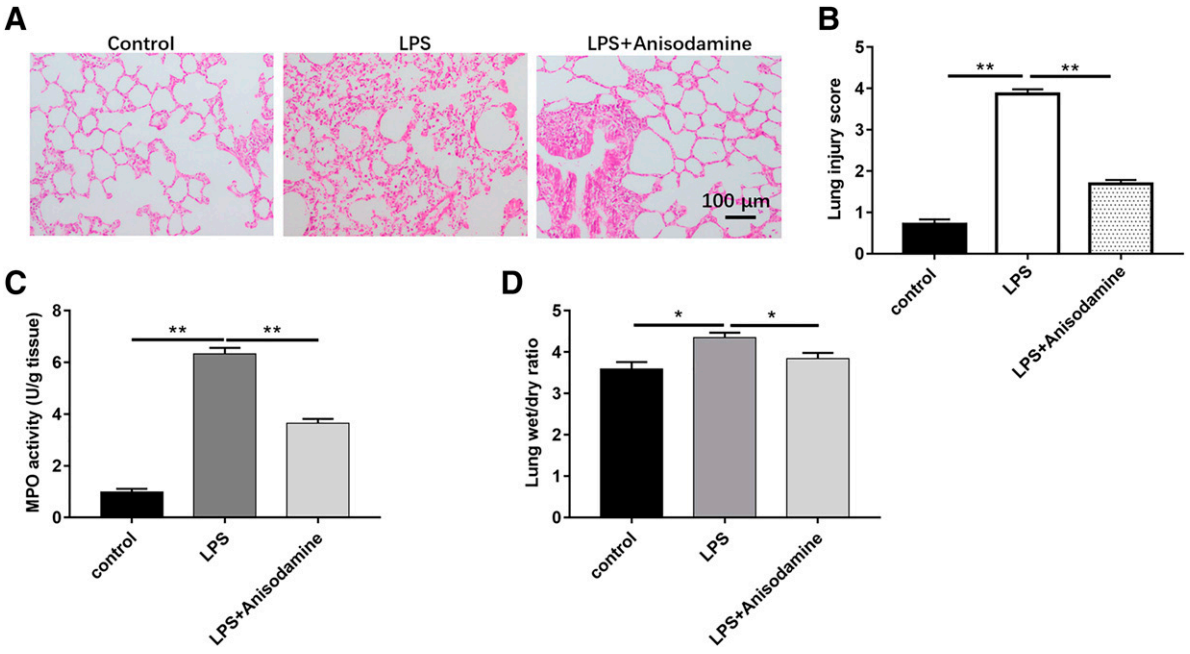

Fig. 1. Anisodamine alleviates LPS-induced ALI. (A) Representative lung histologic changes were assessed with H&E staining after LPS inhalation alone or together with anisodamine treatment. The amplification was 100×. (B) Histologic scores of lungs. (C) MPO activity was detected after LPS inhalation alone or together with anisodamine treatment. (D) Lung wet/dry ratio was detected. Values are presented as mean ± S.E.M. The number of biologic and technical replicates is 8 and that of independent experiments is 3. $^{**}P < 0.05$ compared with control or LPS groups.

established by intranasal instillation of LPS (20 μg/mouse in 100 μL PBS) as described in a previous study (Li et al., 2016). As for anisodamine treatment, mice were intraperitoneally injected with anisodamine (1 mg/kg, Sinopharm, China). G9a overexpression vector, IRF4 shRNA, and corresponding negative controls (empty vector and scrambled shRNA) were injected intraperitoneally into mice at a dose of 2 mg/kg. Lung tissues and bronchoalveolar lavage fluid (BALF) were obtained for analysis at 24 hours after LPS administration. The mice were euthanized by intraperitoneal injection with pentobarbital sodium at a dose of 100 mg/kg. The protocols were approved by the Institutional Animal Care and Use committees of the First Affiliated Hospital of Xi'an Jiaotong University (XJTULAC-2019-173). This study was approved by the Key Research and Development Projects in Shaanxi Province (No. 2020SF-114).

Preparation of Pulmonary Single-Cell Suspensions. Lung tissues collected in this study were washed with PBS, cut into small pieces, and then digested with 0.25% pancreatin for 30 minutes. Then, the digested tissue was vigorously shaken and passed through a 70-μm cell strainer (BD Biosciences). After that, cell suspension was lysed with red blood cell lysis buffer (Beyotime, Shanghai, China), depleted of erythrocytes, and stained followed by flow cytometry analysis.

Flow Cytometry Analysis. After administration with LPS, mice were euthanized with 150 mg/kg pentobarbital sodium, and the bronchoalveolar were washed repeatedly with PBS three times. The collected BALF was placed in a six-well plate, and AMs were obtained by adherence. Then, AMs were collected with Accutase cell detachment solution (Sigma) and were incubated in fluorescence-activated cell sorting buffer (BD Biosciences) under the dark conditions. AMs were sequentially stained with fluorescently labeled antibodies against the following mouse proteins: F4/80, iNOS (ab283655, 1:600, Abcam), and CD206 antibody (141712, 1:100, Biolegend). After being centrifuged at the condition of 350 × g at 4°C for 5 minutes, the AMs were resuspended in fluorescence-activated cell sorting buffer and then subjected to an Accuri C6 flow cytometer (BD Biosciences). All plots shown on populations were gated on lymphocytes by forward and side scattering. Excitation and emission wavelengths were 480 nm and 640 nm, respectively. Each flow cytometric analysis was run on at least 100 000 cells, and FlowJo X was used for the data analysis.

Measurement of Total Cells and Protein Content in BALF. The collected BALF were centrifuged at 1000 rpm for 10 minutes at 4°C. PBS solution was used to resuspend the cell pellets, and a hemocytometer was applied to count the cell number. BALF was added with lysis buffer to lyse red blood cells, and the supernatant was collected. Next, the total protein concentration was detected in BALF by using a BCA protein assay kit (Beyotime, Shanghai, China).

MPO Activity Assay. The obtained lung tissues were homogenized in the buffer that were supplemented with 0.5% hexadecyl-trimethylammonium bromide and 50 mM phosphate. After centrifugation, we

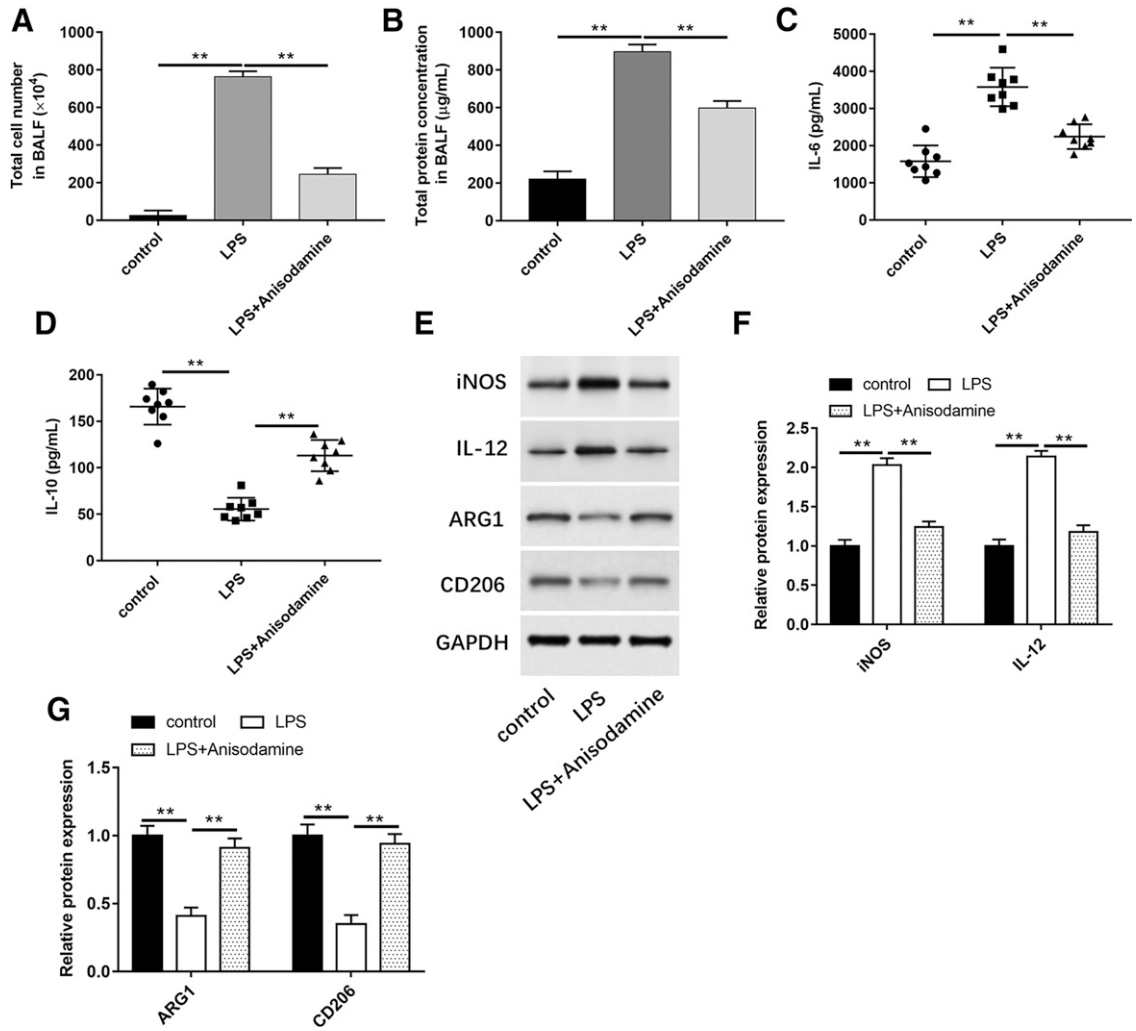

Fig. 2. Anisodamine treatment reverses LPS-induced alterations of M1 macrophages and inflammation cytokine expression. BALF total cell number (A) and protein concentrations (B) were assessed after LPS inhalation alone or together with anisodamine treatment. IL-6 (C) and IL-10 (D) levels were detected with ELISA assay after LPS inhalation alone or together with anisodamine treatment. (E–G) Protein expression of iNOS, IL-12, ARG1, and CD206 were measured with western blotting. Values are presented as mean ± S.E.M. The number of biologic and technical replicates is 8 and that of independent experiments is 3. $^{**}P < 0.05$ compared with sham or control groups.

collected the supernatant and measured the protein concentration with a BCA protein assay kit (Beyotime). Then, 3,30,5,50-tetramethylbenzidine was added followed by the detection of optical density values at 655 nm. The activity of myeloperoxidase (MPO) was measured as the absorbance change per min per milligram protein.

H&E Staining Assay. Lung tissues were fixed in 4% paraformaldehyde overnight, embedded in paraffin, and cut into 5-μm sections. After being stained with H&E (Synthgene, Nanjing, China] for at room temperature, the tissue sections were observed with an optical microscope (Olympus, Tokyo, Japan). Lung histologic damage indexes were evaluated and graded from 0 (normal) to 4 (severe) in four categories in a blinded manner as described in the previous method (Nie et al., 2019).

Culture of BMDMs and Macrophage Polarization. Bone marrow–derived macrophages (BMDMs) were isolated from C57/BL/6J mice as described previously (Zhang et al., 2019). In brief, after the mice were euthanized by rapid cervical dislocation, bone marrow cell suspensions were collected and centrifuged at 500 g for 10 minutes at room temperature. Then, red blood cell lysate (Beckman) was added. After lysis was completed, cells were centrifuged and resuspended in Iscove's modified Dulbecco's medium (Gibco) supplemented with 10% FBS (Gibco), 1% penicillin and streptomycin, and 20 ng/mL macrophage colony–stimulating factor (Prospec). On day 7, the adherent cells became 95% pure macrophages. The presence of the cell surface marker F4/80 was confirmed. Cells were stimulated with 100 ng/mL LPS for 6 hours or 10 ng/mL IL-4 for 24 hours.

ELISA. The concentrations of IL-6 and IL-10 in BALF, cell culture supernatant, or the lung tissues were detected with the ELISA kits (Millipore, Boston) under the manufacturer's recommendations. After the collection of lung tissues and BALF at 24 hours, lung tissues were homogenized and centrifugated, and BALF was centrifuged at 4°C at 500 g for 10 minutes to obtain the respective supernatant for ELISA analysis. In the in vitro BMDM experiments, the cell supernatant was obtained after the indicated treatment to apply for the ELISA detection.

Lung Wet/Dry Weight Ratio. The lung organs of each group were obtained, and the weight was measured on the scale after cleaning the blood stains on the surface, which was considered as the wet weight of lungs. Then, lungs were dried at 70°C for 48 hours, and the dry weight was analyzed until the weight was constant. The wet/dry weight ratio = (wet weight − dry weight)/dry weight.

RT-qPCR Analysis. Total RNA was isolated from BMDMs with TRIzol reagent (Invitrogen, Thermo Fisher Scientific). Isolated RNA

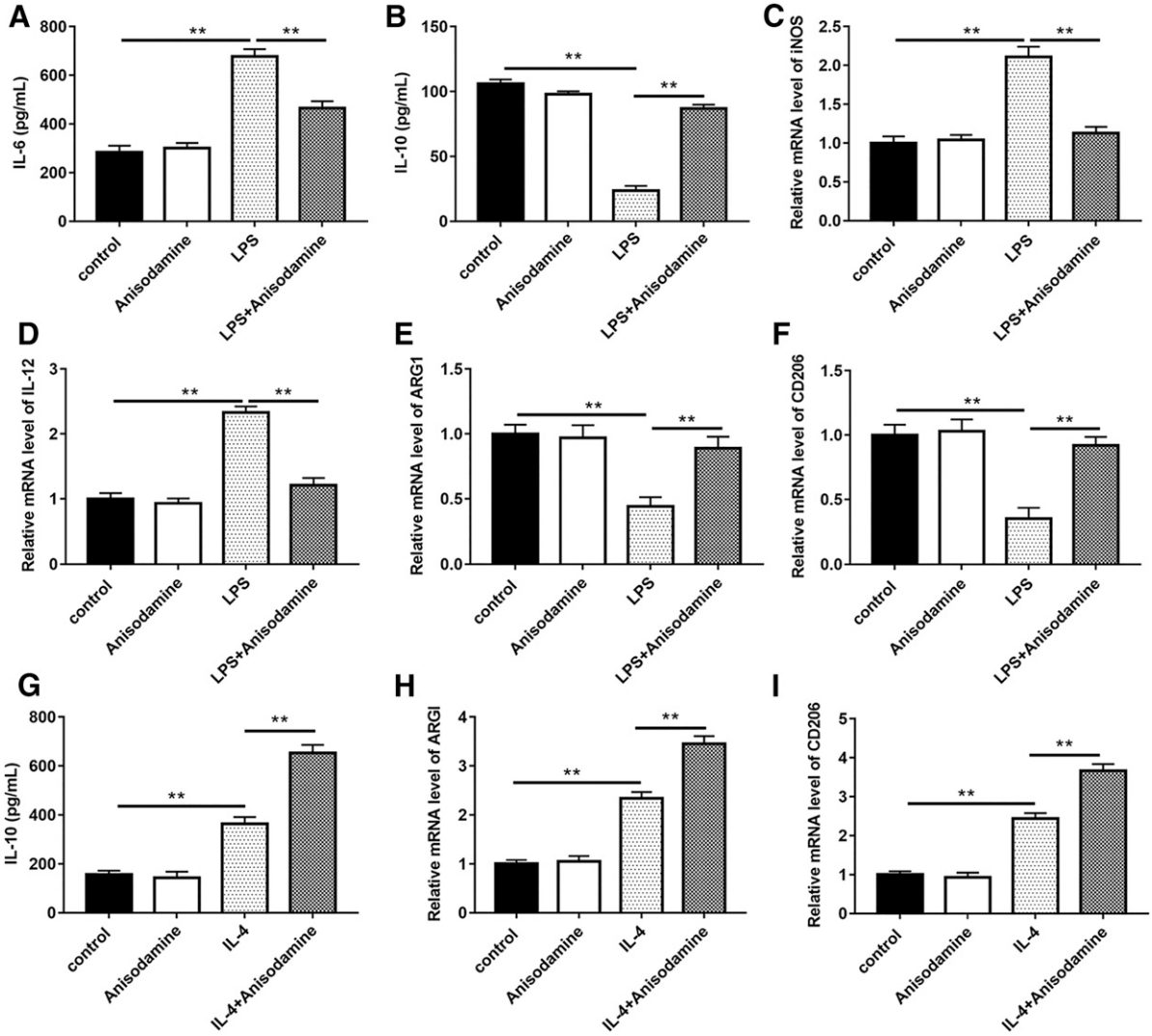

Fig. 3. Anisodamine prevents the alterations of M1 and M2 polarization in LPS-induced BMDMs. BMDMs were treated with anisodamine and/or 100 ng/mL LPS to induce M1 polarization or 10 ng/mL IL-4 to induce M2 polarization. IL-6 (A) and IL-10 (B) levels were detected with ELISA assay after anisodamine and/or LPS treatment. iNOS (C), IL-12 (D), ARG1 (E), and CD206 (F) were analyzed with qPCR anisodamine and/or LPS treatment. IL-10 (G), ARG1 (H), and CD206 (I) levels were detected after anisodamine and/or IL-4 treatment. Values are presented as mean ± S.E.M. The number of biologic and technical replicates is 4 and that of independent experiments is 3 times. $^{**}P < 0.05$ compared with control, LPS, or IL-4 groups.

was reversely transcribed into cDNA with PrimeScript RT reagent Kit (Takara, Dalian, China), and RT-qPCR was conducted with the SYBR Premix Ex Taq II (Takara) on an ABI 7500 Real-Time PCR System (Applied Biosystems, Foster City). The PCR parameters were performed at 95°C for 30 seconds, followed by 30 cycles of 95°C for 5 seconds, then 60°C for 30 seconds and 72°C for 15 second. PCR reaction system contained 12.5 μL of SYBR Premix Ex Taq II, 1.0 μL of RT primer, 1 μL of cDNA sample, and 10.5 μL of double-distilled H_2O. The relative expression levels were calculated by the $2^{-\Delta\Delta CT}$ method and normalized to glyceraldehyde-3-phosphate dehydrogenase. The primer sequences used in this study are provided in Supplemental Table 1.

Western Blotting. Total proteins from lung tissues or BMDMs were extracted with RIPA lysis buffer (Beyotime). Then, cell lysates and lung homogenates were centrifuged at 10 000 g for 25 minutes and then 15 000 g for 20 minutes, respectively. The protein concentration was measured using a BCA protein assay kit (Beyotime, Shanghai, China). Protein samples were separated on SDS-polyacrylamide gels and then transferred onto PVDF membranes. After that, the membranes were blocked with 5% skim milk for 1 hour at room temperature and then incubated with primary antibodies against the following proteins overnight at 4°C: iNOS (ab178945, 1:2000, Abcam), IL-12 (ab131156, 1:10,0000, Abcam), ARG1 (ab203490, 1:3000, Abcam), CD206 (ab64693, 1:3000, Abcam), G9a (ab229455, 1:3000, Abcam), histone-3-lysine (H3K)-9me2 (ab1220, 1:5000, Abcam), H3 (ab1791, 1:4000, Abcam), and IRF4 (ab133590, 1:50000, Abcam). The next day, a horseradish peroxidase–conjugated secondary antibody (1:500 dilution, ab6721, Abcam) was added and incubated for 1 hour at 37°C. Protein bands were analyzed with a chemiluminescence imaging system (Oxiang, Shanghai, China).

Statistical Analysis. The data are presented as the mean ± S.E.M. Data comparisons between multiple groups were analyzed using ANOVA, and data between two groups were analyzed using Student's *t* tests. ANOVA was followed by Duncan, SNK, or other methods for pairwise comparisons if the overall means of the groups were not equal. Our analysis showed that the data were normally distributed and variances were homogeneous. Hence, the ANOVA followed by Duncan test was used to determine the differences among groups. *P* values less than 0.05 were considered significant.

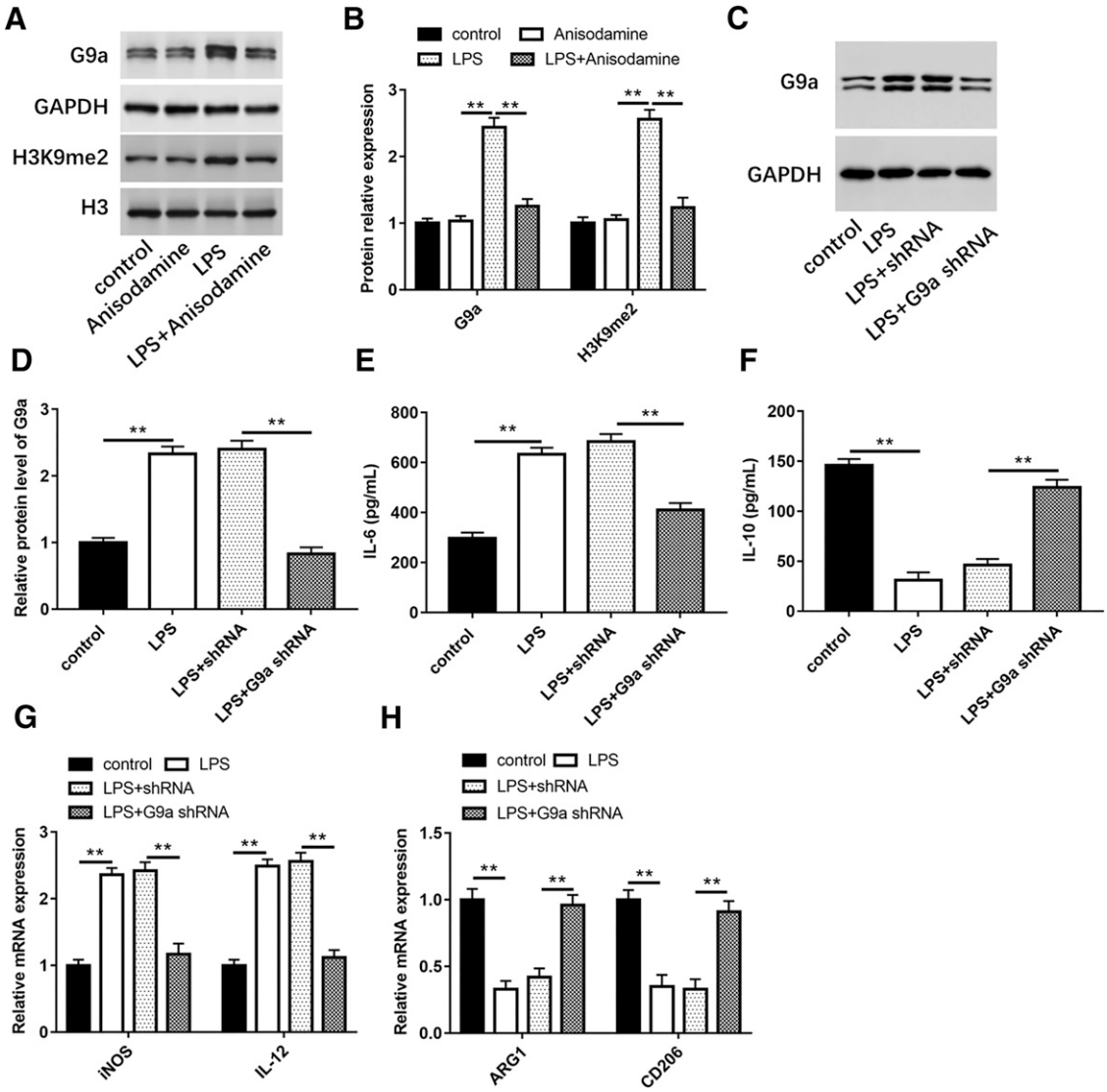

Fig. 4. G9a and H3K9 methylation are elevated by LPS, and silence of G9a reverses the alterations of M2 polarization in LPS-induced BMDMs. (A and B) Protein expression of G9a and H3K9me2 was analyzed in BMDMs treated with LPS and anisodamine separately or jointly. (C and D) Protein level of G9a after transfection with G9a shRNA. The levels of IL-6 (E) and IL-10 (F) were detected with ELISA. The mRNA levels of M1 polarization markers (G) and M2 polarization markers (H) were analyzed with RT-qPCR. Values are presented as mean ± S.E.M. The number of biologic and technical replicates is 4 and that of independent experiments is 3. $^{**}P < 0.05$ compared with control, anisodamine, or LPS + shRNA groups.

Results

Anisodamine Alleviates LPS-Induced ALI. After the mice were treated with LPS, the lung architecture was significantly damaged, accompanied with lung edema and hemorrhage as compared with the control group (Fig. 1, A and B; $P < 0.05$). LPS treatment increased the MPO activity (Fig. 1C; $P < 0.05$), which suggested that LPS increased the neutrophil infiltration in lung tissues. Furthermore, the wet/dry ratio was detected to evaluate the severity of pulmonary edema, and we found that lung wet/dry ratio was markedly promoted in the LPS group (Fig. 1D, $P < 0.05$). However, anisodamine treatment weakened lung damage induced by LPS and reversed the promoting influences of LPS on MPO activity and lung wet/dry ratio ($P < 0.05$).

Anisodamine Blocks LPS-Induced M1 Polarization of Macrophages and Inflammatory Cytokine Expression in ALI Mice. To explore whether anisodamine attenuates lung injury through macrophages, the total cell number and protein concentrations in BALF were detected. Compared with the LPS group, anisodamine treatment significantly reduced cell number and protein concentrations in BALF (Fig. 2, A and B; $P < 0.05$). Moreover, anisodamine treatment inhibited IL-6 level and the levels of iNOS and IL-12 proteins in lung tissues, whereas it increased IL-10 level and levels of ARG1 and CD206 proteins (Fig. 2, C–G; $P < 0.05$).

Anisodamine Prevents the Alterations of M1 Polarization and M2 Polarization in LPS-Induced BMDMs. BMDMs were stimulated with anisodamine and/or 100 ng/mL LPS to induce M1 polarization or 10 ng/mL IL-4 to induce M2 polarization. After BMDMs were stimulated with LPS, we found the secretion of IL-6 and the expression of M1 markers iNOS and IL-12 were dramatically increased, whereas IL-10, ARG1, and CD206 (M2 markers) levels were notably reduced (Fig. 3, A–F; $P < 0.05$). The levels of IL-10 and M2 polarization markers were significantly elevated in BMDMs stimulated with IL-4 (Fig. 3, G–I; $P < 0.05$). However, anisodamine weakened the promoting effects of LPS on IL-6 and M1 polarization marker levels and the inhibitory effects of IL-10 and M2 polarization marker levels, further enhancing the levels of IL-10 and M2 polarization markers in IL-4–stimulated cells ($P < 0.05$).

G9a and H3K9 Methylation Are Elevated by LPS, and Silence of G9a Suppresses the Alterations of M1 and M2 Polarization in BMDMs Induced by LPS. The protein expression levels of G9a, H3K9me2 were increased after LPS stimulated, whereas anisodamine treatment reversed the promoting effects (Fig. 4, A and B; $P < 0.05$). Then, BMDMs were transfected with G9a shRNA before LPS treatment. The protein level of G9a was observably inhibited after G9a silence in LPS-stimulated cells (Fig. 4, C and D; $P < 0.05$). Furthermore, the level of IL-6 and the mRNA levels of iNOS and IL-12 were remarkably reduced after the knockdown of G9a, whereas IL-10 level and the mRNA levels of ARG1 and CD206 were significantly elevated (Fig. 4, E–H; $P < 0.05$).

G9a Directly Interacts with the IRF4 Gene Promoter. To explore whether G9a effected inflammatory factor levels and macrophage polarization via modulating IRF4, chromatin immunoprecipitation assay was conducted. We found

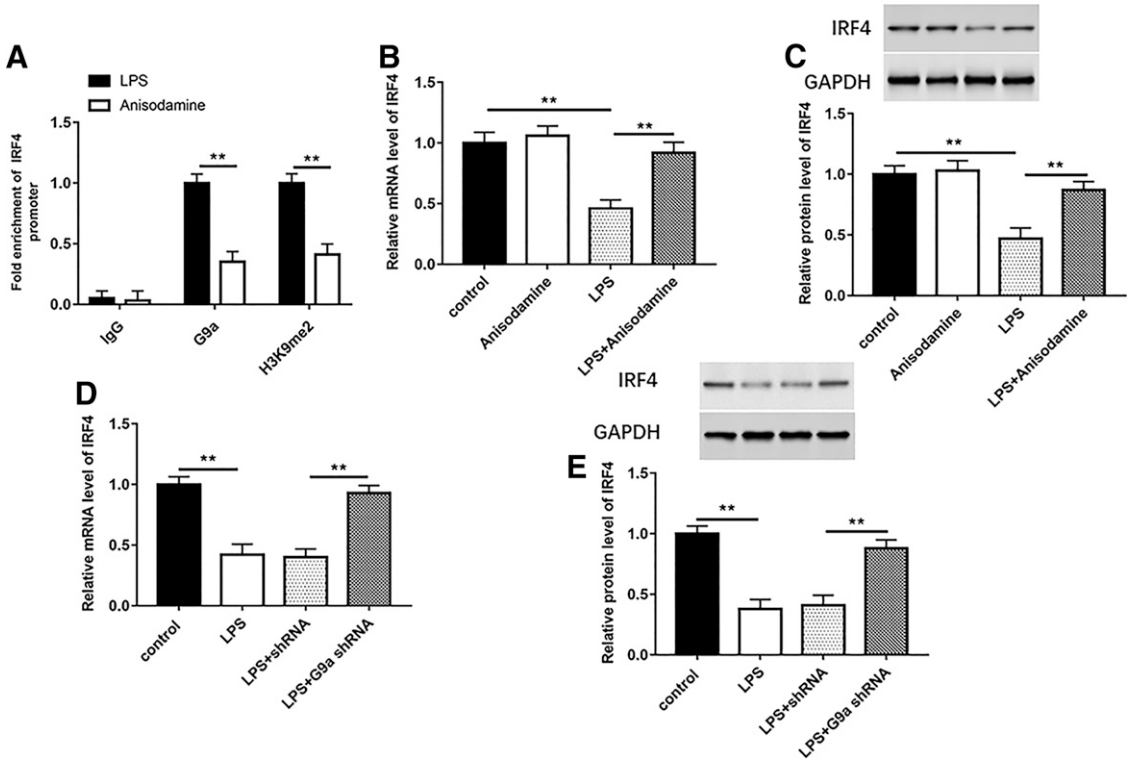

Fig. 5. G9a directly interacts with the IRF4 gene promoter. (A) ChIP assay was conducted to verify the binding of G9a to IRF4 promoter. (B) The mRNA level of IRF4 was analyzed after BMDMs were treated with LPS and anisodamine separately or jointly. (C) The protein level of IRF4 was measured after BMDMs were treated with LPS and anisodamine separately or jointly. (D) The mRNA level of IRF4 was analyzed after BMDMs were treated with LPS and/or transfected with G9a shRNA. (E) Western blotting was performed to detect the protein level of IRF4 after BMDMs were treated with LPS and/or transfected with G9a shRNA. Values are presented as mean ± S.E.M. The number of biologic and technical replicates is 4 and that of independent experiments is 3. $^{**}P < 0.05$ compared with control, LPS, or LPS + shRNA groups. ChIP, chromatin immunoprecipitation.

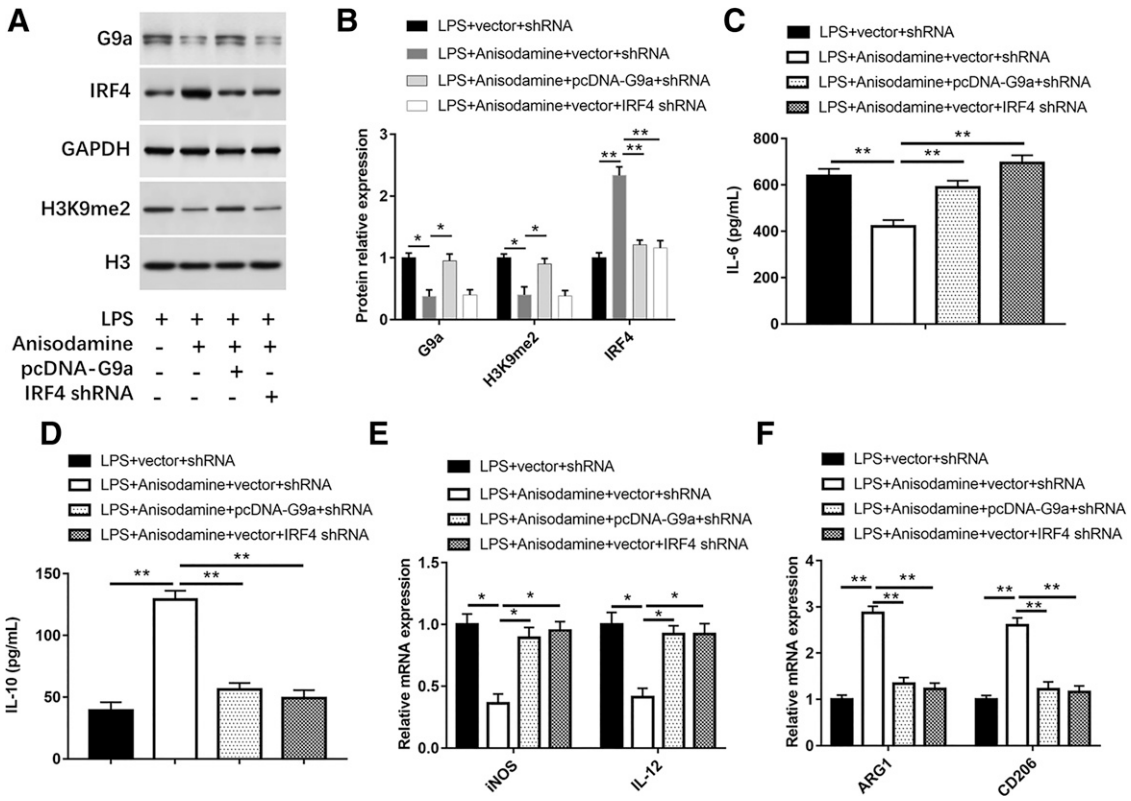

Fig. 6. Overexpression of G9a or silence of IRF4 reverses the effect of anisodamine on the alterations of M2 polarization in LPS-induced BMDMs. BMDMs were transfected with G9a overexpression vector and/or IRF4 shRNA before LPS treatment. (A and B) Protein expression levels of G9a, H3K9me2, and IRF42 were analyzed. The levels of IL-6 (C) and IL-10 (D) were detected with ELISA assay. The mRNA levels of M1 polarization markers (E) and M2 polarization markers (F) were analyzed with qPCR. Values are presented as mean ± S.E.M. The number of biologic and technical replicates is 4 and that of independent experiments is 3. $^{**}P < 0.05$ compared with LPS + vector + shRNA or LPS + anisodamine + vector + shRNA groups.

that anisodamine administration promoted the binding of G9a and H3K9me2 to the IRF4 promoter (Fig. 5A; $P < 0.05$). Moreover, anisodamine treatment dramatically promoted the expression of IRF4 at mRNA and protein levels as compared with the LPS treatment (Fig. 5, B and C; $P < 0.05$). Furthermore, downregulation of G9a could also elevate the expression of IRF4 in BMDMs after the stimulation of LPS (Fig. 5, D and E; $P < 0.05$).

Overexpression of G9a or Silence of IRF4 Reversed the Effect of Anisodamine on the Alterations of M1 and M2 Polarization in LPS-Induced BMDMs. To further observe the functions of G9a and IRF4 in the regulation of macrophage polarization, BMDMs were transfected with pcDNA-G9a or IRF4 shRNA before LPS and anisodamine treatment. Compared with the LPS treatment group, the protein expression of G9a and H3K9me2, the concentration of IL-6, and the levels of iNOS and IL-12 were decreased by anisodamine treatment, whereas the IRF4 protein expression, IL-10 level, and the levels of ARG1 and CD206 expression were markedly improved (Fig. 6; $P < 0.05$). However, overexpression of G9a or silence of IRF4 could reverse all the effects of anisodamine ($P < 0.05$).

Overexpression of G9a or Silence of IRF4 Weakened the Protective Effect of Anisodamine on LPS-Induced ALI. Mice were injected with lentiviral vectors expressing G9a gene or IRF4 shRNA before LPS and anisodamine treatment. The results of H&E staining revealed that overexpression of G9a or silence of IRF4 could reverse the improvement of anisodamine on lung injury (Fig. 7, A and B; $P < 0.05$). Moreover, overexpression of G9a or IRF4 silence reversed the inhibitory effects of anisodamine on MPO activity, IL-6 level, the protein levels of G9a and H3K9me2, and the promoting effect of IL-10 level and IRF4 protein expression (Fig. 7, C–E and I; $P < 0.05$). We observed that the percentages of $F4/80^+$ $iNOS^+$ alveolar macrophages were significantly increased, whereas $F4/80^+$ $CD206^+$ M2 alveolar macrophages decreased after LPS injection (Fig. 7, F–H; $P < 0.05$). Anisodamine treatment reversed the LPS-induced increase in M1 phenotype and decrease in M2 phenotype ($P < 0.05$). However, overexpression of G9a or silence of IRF4 observably reversed the effects of anisodamine ($P < 0.05$).

Thus, anisodamine treatment could inhibit the expression of G9a, which decreased the binding of G9a and H3K9me2 to the IRF4 promoter, thus enhancing the expression of IRF4. Upregulation of IRF4 suppressed the LPS-induced alterations of M1 and promoted the alterations of IL-4–induced M2 polarization, which alleviated LPS-induced ALI (Fig. 8).

Discussion

Anisodamine was reported to inhibit inflammatory processes in acute kidney injury and pancreatic acinar cell injury (Yuan et al., 2017; Li et al., 2020b). In this study, our data demonstrated that anisodamine inhibited lung injury and cell apoptosis resulting from LPS stimulation and alleviated lung

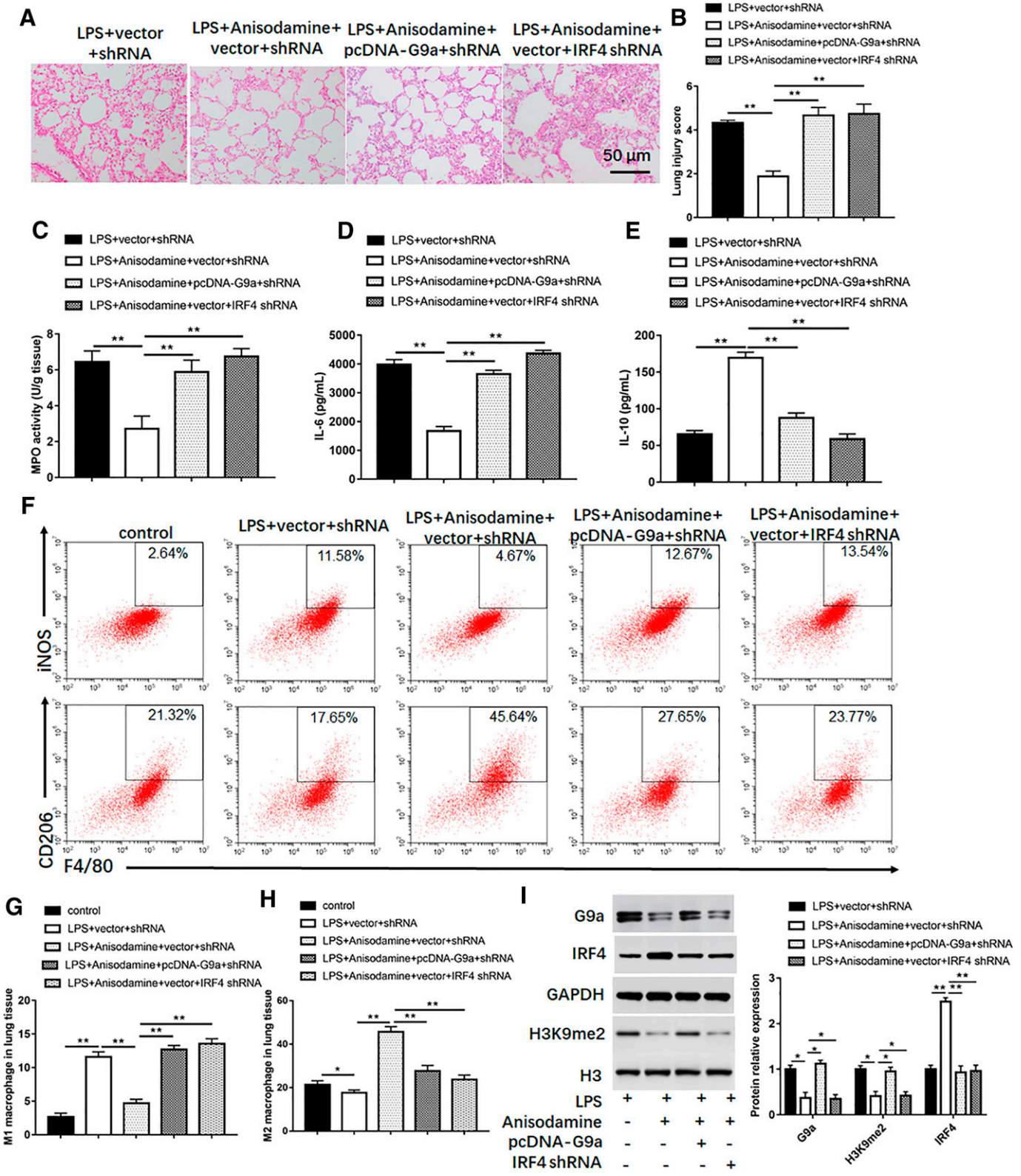

Fig. 7. Overexpression of G9a or silence of IRF4 reverses the effect of anisodamine on the improvement of LPS-induced ALI. (A) Representative H&E staining images of lung histologic changes before and after LPS inhalation. The amplification was 100×. (B) Lung score was evaluated. (C) MPO activity was detected after LPS inhalation. IL-6 (D) and IL-10 (E) levels were analyzed with ELISA. (F) Flow cytometry analysis for the percentage of F4/80 + iNOS + M1 alveolar macrophages and F4/80 + CD206 + M2 macrophages. Quantification of flow cytometry of F4/80 + iNOS + M1 alveolar macrophages (G) and F4/80 + CD206 + M2 macrophages (H). (I) Protein levels of G9a, H3K9me2, and IRF4 were detected. Values are presented as mean ± S.E.M. The number of biologic and technical replicates is 8 and that of independent experiments is 3. $^{**}P < 0.05$ compared with control, LPS + vector + shRNA or LPS + anisodamine + vector + shRNA groups.

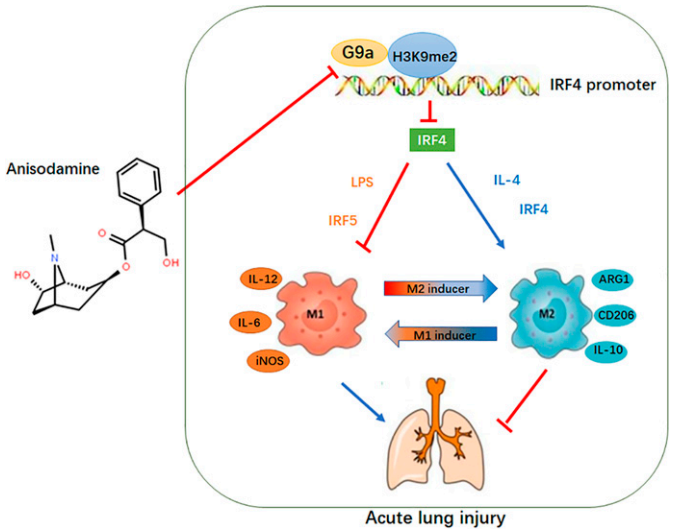

Fig. 8. A schematic diagram for the protective effects of anisodamine against LPS-induced ALI through the G9a/IRF4 axis. Anisodamine treatment could inhibit the expression of G9a, which decreased the binding of G9a and H3K9me2 to the IRF4 promoter, thus enhancing the expression of IRF4. Upregulation of IRF4 suppressed the LPS-induced alterations of M1 and promoted the alterations of IL-4–induced M2 polarization to alleviate LPS-induced ALI. Blue arrows represent promoting events. Red perpendicular bars represent inhibitory events.

edema, and the specific mechanism was that anisodamine inhibited LPS-induced alterations of M1 and M2 macrophage polarization.

Transcription factors are considered as the key molecules to determine expression of specific genes in macrophages, and as a result, the activation of specific transcription factors is an important factor in the occurrence of macrophage dynamics (Li et al., 2018b). For example, signal transducers and activators of transcription (STAT) 1, CCAAT/enhancer binding protein α, Kruppel-like factor (KLF) 6, and nuclear factor-kappa B are important transcription factors, which are demonstrated to regulate the M1 macrophage polarization, where peroxisome proliferator activated receptors, STAT3/6, and c-MYC have been implicated in M2 macrophage polarization (Molawi and Sieweke, 2013; Tugal et al., 2013). Ginsenosides significantly decreased the secretion of inflammatory factors resulting from LPS stimulation via suppressing the activation of STAT1 with TLR4 (Huynh et al., 2020). Inhibition of miR-34a significantly ameliorated lung injury and inflammation caused by LPS treatment via upregulation of KLF4 and promotion of the alterations of M2 phenotype (Khan et al., 2020).

As key regulatory transcription factors of the interferon signaling pathway, IRFs play important regulatory roles in cell immunity, cell differentiation, tumor regulation, and stress responses, and as such, in the differentiation and polarization of macrophages (Chistiakov et al., 2018). IRF1-5 and IRF-8 have been implicated in the macrophage polarization. IRF-3 plays a critical role in the differentiation of monocyte macrophage stimulated by macrophage colony–stimulating factor, IRF-4 contributes to M1 macrophage polarization, and IRF-5 is a crucial factor for M2 macrophage polarization (Ferrante and Leibovich, 2012; Günthner and Anders, 2013). IRF4, a hematopoietic specific transcription factor, regulates the maturation of lymphocytes, myeloid cells, and dendritic cells and represses inflammation development (Yanai et al., 2012). Downregulation of IRF5 promoted the expression of IRF4, contributed to the activation of M2, suppressed the production of inflammatory factors, and alleviated stroke prognosis, whereas IRF4 knockdown elevated the expression level of IRF5, promoted the activation of M1, and heightened inflammatory responses (Al Mamun et al., 2020). Our study revealed that anisodamine treatment increased the mRNA and protein expression levels of IRF4 in LPS-induced BMDMs and restored the inhibitory effect of LPS on M2 polarization. Downregulation of IRF4 could reverse the promoting effect of anisodamine on the alterations of M2 polarization.

Under pathophysiological conditions, the alterations of phenotype and function in M1 and M2 macrophages were observed along with the changes of signaling molecules, transcription factors, epigenetic regulators, and cellular metabolism (Wang et al., 2020). Orphan nuclear receptors retinoic acid–related orphan receptors α, which can participate in the M1/M2 polarization of liver host Kupffer cells, enhanced M2 polarization by inducing KLF4 (Han et al., 2017).

Epigenetic regulation may participate in macrophage polarization through modulating the related genes. Histone modifications, particularly in the N-terminal tail, are reported to be critical factors in controlling gene sets (Medzhitov and Horng, 2009). In the case of histone modifications, H3K9 is associated with the silence of gene expression. Jumonji domain–containing-3 is considered as a H3K27 demethylase promoting IRF4 expression to activate M2 macrophage (Satoh et al., 2010). G9a, a widely expressed histone methyltransferase, catalyzes mono- and dimethylation of histone H3K9 (H3K9me1 and H3K9me2), which are associated with transcriptional activation and repression, respectively (Ebbers et al., 2016). The G9a-specific inhibitor BIX01294 blocks spinal nerve injury or chronic constriction injury–induced H3K9me2 levels, a marker of G9a activity, thereby reducing pain hypersensitivity development (Liang et al., 2019). In fibroblasts, inhibition of the Chromebox homolog 5/G9a pathway enhances the modification of H3K9 methylation and decreases the accumulation of collagen in the lung after bleomycin injury (Ligresti et al., 2019). Our study revealed that anisodamine suppressed G9a and H3K9me2 protein levels, whereas it increased IRF4 protein level, indicating that anisodamine alleviated ALI through suppressing G9a-mediated IRF4 silence.

In summary, using mouse BMDMs to examine what role the anisodamine played in macrophage polarization under polarizing conditions in vitro, we found that anisodamine remarkably suppressed the alterations of M1 polarization caused by LPS treatment, whereas it enhanced the alterations of M2 polarization. In ALI mouse models, anisodamine treatment was able to alleviate LPS-induced lung injury and pulmonary edema through reversing the alterations of LPS-induced M1 and M2 polarization by inhibiting G9a-mediated silence of IRF4, which provided a potential strategy to improve ALI.

Authorship Contributions

Participated in research design: Du, Tang.
Conducted experiments: Zhang, Song, Peng, Wang.
Performed data analysis: Song, Peng, Wang, Li, Ren, Sun.
Wrote or contributed to the writing of the manuscript: Zhang, Du, Tang.

References

Al Mamun A, Chauhan A, Qi S, Ngwa C, Xu Y, Sharmeen R, Hazen AL, Li J, Aronowski JA, McCullough LD et al. (2020) Microglial IRF5-IRF4 regulatory axis regulates

neuroinflammation after cerebral ischemia and impacts stroke outcomes. *Proc Natl Acad Sci USA* **117**:1742–1752.
Chistiakov DA, Myasoedova VA, Revin VV, Orekhov AN, and Bobryshev YV (2018) The impact of interferon-regulatory factors to macrophage differentiation and polarization into M1 and M2. *Immunobiology* **223**:101–111.
Ebbers L, Runge K, and Nothwang HG (2016) Differential patterns of histone methylase EHMT2 and its catalyzed histone modifications H3K9me1 and H3K9me2 during maturation of central auditory system. *Cell Tissue Res* **365**:247–264.
Ferrante CJ and Leibovich SJ (2012) Regulation of Macrophage Polarization and Wound Healing. *Adv Wound Care (New Rochelle)* **1**:10–16.
Günthner R and Anders HJ (2013) Interferon-regulatory factors determine macrophage phenotype polarization. *Mediators Inflamm* **2013**:731023.
Guoshou Z, Chengye Z, Zhihui L, and Jinlong L (2013) Effects of high dose of anisodamine on the respiratory function of patients with traumatic acute lung injury. *Cell Biochem Biophys* **66**:365–369.
Han YH, Kim HJ, Na H, Nam MW, Kim JY, Kim JS, Koo SH, and Lee MO (2017) RORα Induces KLF4-Mediated M2 Polarization in the Liver Macrophages that Protect against Nonalcoholic Steatohepatitis. *Cell Rep* **20**:124–135.
Huang X, Xiu H, Zhang S, and Zhang G (2018) The Role of Macrophages in the Pathogenesis of ALI/ARDS. *Mediators Inflamm* **2018**:1264913.
Huynh DTN, Baek N, Sim S, Myung CS, and Heo KS (2020) Minor Ginsenoside Rg2 and Rh1 Attenuates LPS-Induced Acute Liver and Kidney Damages via Downregulating Activation of TLR4-STAT1 and Inflammatory Cytokine Production in Macrophages. *Int J Mol Sci* **21**:6656.
Khan MJ, Singh P, Dohare R, Jha R, Rahmani AH, Almatroodi SA, Ali S, and Syed MA (2020) Inhibition of miRNA-34a Promotes M2 Macrophage Polarization and Improves LPS-Induced Lung Injury by Targeting Klf4. *Genes (Basel)* **11**:966.
Laskin DL, Malaviya R and Laskin JD (2019) Role of Macrophages in Acute Lung Injury and Chronic Fibrosis Induced by Pulmonary Toxicants. *Toxicol Sci* **168**:287–301.
Li D, Ren W, Jiang Z, and Zhu L (2018a) Regulation of the NLRP3 inflammasome and macrophage pyroptosis by the p38 MAPK signaling pathway in a mouse model of acute lung injury. *Mol Med Rep* **18**:4399–4409.
Li H, Jiang T, Li MQ, Zheng XL, and Zhao GJ (2018b) Transcriptional Regulation of Macrophages Polarization by MicroRNAs. *Front Immunol* **9**:1175.
Li P, Liu Y, and He Q (2020a) Anisodamine Suppressed the Growth of Hepatocellular Carcinoma Cells, Induced Apoptosis and Regulated the Levels of Inflammatory Factors by Inhibiting NLRP3 Inflammasome Activation. *Drug Des Devel Ther* **14**:1609–1620.
Li Y, Huang J, Foley NM, Xu Y, Li YP, Pan J, Redmond HP, Wang JH, and Wang J (2016) B7H3 ameliorates LPS-induced acute lung injury via attenuation of neutrophil migration and infiltration. *Sci Rep* **6**:31284.
Li Z, Xu C, Tao Y, Liang Y, Liang Q, Li J, Li R, and Ye H (2020b) Anisodamine alleviates lipopolysaccharide-induced pancreatic acinar cell injury through NLRP3 inflammasome and NF-κB signaling pathway. *J Recept Signal Transduct Res* **40**:58–66.
Liang L, Zhao JY, Kathryn T, Bekker A, and Tao YX (2019) BIX01294, a G9a inhibitor, alleviates nerve injury-induced pain hypersensitivities during both development and maintenance periods. *Transl Perioper Pain Med* **6**:106–114.
Ligresti G, Caporarello N, Meridew JA, Jones DL, Tan Q, Choi KM, Haak AJ, Aravamudhan A, Roden AC, Prakash YS et al. (2019) CBX5/G9a/H3K9me-mediated gene repression is essential to fibroblast activation during lung fibrosis. *JCI Insight* **5**:e127111.
Lin F, Song C, Zeng Y, Li Y, Li H, Liu B, Dai M, and Pan P (2020) Canagliflozin alleviates LPS-induced acute lung injury by modulating alveolar macrophage polarization. *Int Immunopharmacol* **88**:106969.
Medzhitov R and Horng T (2009) Transcriptional control of the inflammatory response. *Nat Rev Immunol* **9**:692–703.
Molawi K and Sieweke MH (2013) Transcriptional control of macrophage identity, self-renewal, and function. *Adv Immunol* **120**:269–300.
Nie Y, Wang Z, Chai G, Xiong Y, Li B, Zhang H, Xin R, Qian X, Tang Z, Wu J et al. (2019) Dehydrocostus Lactone Suppresses LPS-induced Acute Lung Injury and Macrophage Activation through NF-κB Signaling Pathway Mediated by p38 MAPK and Akt. *Molecules* **24**:1510.
Qiu P, Liu Y, Chen K, Dong Y, Liu S, and Zhang J (2021) Hydrogen-rich saline regulates the polarization and apoptosis of alveolar macrophages and attenuates lung injury via suppression of autophagy in septic rats. *Ann Transl Med* **9**:974.
Ren AQ, Wang HJ, Zhu HY, Ye G, Li K, Chen DF, Zeng T, and Li H (2021) Glycoproteins From *Rabdosia japonica* var. *glaucocalyx* Regulate Macrophage Polarization and Alleviate Lipopolysaccharide-Induced Acute Lung Injury in Mice *via* TLR4/NF-κB Pathway. *Front Pharmacol* **12**:693298.
Rőszer T (2015) Understanding the Mysterious M2 Macrophage through Activation Markers and Effector Mechanisms. *Mediators Inflamm* **2015**:816460.
Satoh T, Takeuchi O, Vandenbon A, Yasuda K, Tanaka Y, Kumagai Y, Miyake T, Matsushita K, Okazaki T, Saitoh T et al. (2010) The Jmjd3-Irf4 axis regulates M2 macrophage polarization and host responses against helminth infection. *Nat Immunol* **11**:936–944.
Song C, Li H, Li Y, Dai M, Zhang L, Liu S, Tan H, Deng P, Liu J, Mao Z et al. (2019) NETs promote ALI/ARDS inflammation by regulating alveolar macrophage polarization. *Exp Cell Res* **382**:111486.
Tugal D, Liao X, and Jain MK (2013) Transcriptional control of macrophage polarization. *Arterioscler Thromb Vasc Biol* **33**:1135–1144.
Wang L, Zhang H, Sun L, Gao W, Xiong Y, Ma A, Liu X, Shen L, Li Q, and Yang H (2020) Manipulation of macrophage polarization by peptide-coated gold nanoparticles and its protective effects on acute lung injury. *J Nanobiotechnology* **18**:38.
Wang LX, Zhang SX, Wu HJ, Rong XL, and Guo J (2019) M2b macrophage polarization and its roles in diseases. *J Leukoc Biol* **106**:345–358.
Xie W, Lu Q, Wang K, Lu J, Gu X, Zhu D, Liu F, and Guo Z (2018) miR-34b-5p inhibition attenuates lung inflammation and apoptosis in an LPS-induced acute lung injury mouse model by targeting progranulin. *J Cell Physiol* **233**:6615–6631.
Yanai H, Negishi H, and Taniguchi T (2012) The IRF family of transcription factors: Inception, impact and implications in oncogenesis. *OncoImmunology* **1**:1376–1386.
Yao BJ, He XQ, Lin YH, and Dai WJ (2018) Cardioprotective effects of anisodamine against myocardial ischemia/reperfusion injury through the inhibition of oxidative stress, inflammation and apoptosis. *Mol Med Rep* **17**:1253–1260.
You QH, Zhang D, Niu CC, Zhu ZM, Wang N, Yue Y, and Sun GY (2014) Expression of IL-17A and IL-17F in lipopolysaccharide-induced acute lung injury and the counteraction of anisodamine or methylprednisolone. *Cytokine* **66**:78–86.
Yuan X, Zheng Y, Chen C and Wang C (2017) Anisodamine inhibits endoplasmic reticulum stress-associated TXNIP/NLRP3 inflammasome activation in rhabdomyolysis-induced acute kidney injury. *Apoptosis* **22**:1524–1531.
Zhang W, Zhang Y, He Y, Wang X, and Fang Q (2019) Lipopolysaccharide mediates time-dependent macrophage M1/M2 polarization through the Tim-3/Galectin-9 signalling pathway. *Exp Cell Res* **376**:124–132.
Zhao X, Zhao B, Zhao Y, Zhang Y, and Qian M (2021) Protective effect of anisodamine on bleomycin-induced acute lung injury in immature rats via modulating oxidative stress, inflammation, and cell apoptosis by inhibiting the JAK2/STAT3 pathway. *Ann Transl Med* **9**:859.
Zhou P, Yang XL, Wang XG, Hu B, Zhang L, Zhang W, Si HR, Zhu Y, Li B, Huang CL et al. (2020) A pneumonia outbreak associated with a new coronavirus of probable bat origin. *Nature* **579**:270–273.

Address correspondence to: Dr. Ning Du, Department of Thoracic Surgery, The First Affiliated Hospital of Xi'an Jiaotong University, 277 West Yanta Road, Xi'an 710061, China. E-mail: duning43@21cn.com; or Shou-Ching Tang, Cancer Center and Research Institute, University of Mississippi Medical Center, Guyton Research Building, G-651-07, 2500 North State Street, Jackson, MS 39216. E-mail: tangsc7@21cn.com